Organic Electronics 12 (2011) 2159–2164

Contents lists available at SciVerse ScienceDirect

Organic Electronics

journal homepage: www.elsevier.com/locate/orgel

Widely variable Seebeck coefficient and enhanced thermoelectric power of PEDOT:PSS films by blending thermal decomposable ammonium formate

Tsung-Che Tsai, Hsiu-Cheng Chang, Chun-Hua Chen *, Wha-Tzong Whang *

Department of Materials Science and Engineering, National Chiao Tung University, 1001 Ta-Hsueh Road, Hsin-Chu 30010, Taiwan, ROC

ARTICLE INFO

Article history:
Received 21 April 2011
Received in revised form 25 August 2011
Accepted 11 September 2011
Available online 28 September 2011

Keywords:
Thermoelectric
PEDOT:PSS
Ammonium formate
Seebeck coefficient

ABSTRACT

The doping effects of thermal decomposable ammonium formate (AF) from 5 to 50 wt.% on the electrical conductivity, Seebeck coefficient, and microstructures of poly(3,4-ethylenedioxythiophene):poly(styrenesulfonate) (PEDOT:PSS) films have been investigated for the first time for modern thermoelectric applications. It has been found that the Seebeck coefficient can be effectively tuned in a very wide range by varying the AF doping concentration, where a maximum value of 436.3 μV/K was obtained, i.e., ~40 times higher in magnitude than the pure PEDOT:PSS films prepared with same processes. The greatly enhanced Seebeck coefficient is considered to be the result of reducing the carrier concentration, as evidenced by the Hall measurement. In addition, AF also plays an important role in the formation of the closed or open pores and channels within the films for phonon scattering, as can be clearly observed in the SEM images. The present work provides a new procedure to effectively control the Seebeck coefficient as well as the microstructures of PEDOT:PSS polymer by a simple blending approach with suitable thermal steps, which has not previously been reported.

1. Introduction

In recent years, thermoelectric (TE) materials have become one of the hottest research topics since a series of remarkable breakthroughs in the TE figure of merit (ZT), which mainly originate from the novel nanostructural design [1,2]. This new technique for the first time enables TE technology to approach a level that is comparable with other green-energy systems, and further accelerates the progress in fundamental researches and applications. The ZT value determined for the performance evaluation of TE materials is governed by multiple physical parameters, expressed as:

$$ZT = \frac{\sigma \cdot S^2}{\kappa} T = \frac{P}{\kappa} T \quad (1)$$

where S, T, σ, κ and P are the Seebeck coefficient, absolute temperature, electrical conductivity, thermal conductivity and power factor, respectively [3–6].

Among the various categories of thermoelectric materials, a great deal of attention has recently been given to organic TE materials, particularly since the time when the conducting polymers were discovered. The solubility and flexibility, which allow for either the easy blending or integrating with other organic/inorganic TE materials with simple or unusual topologies, are the most attractive features of the organic TE materials [3]. Furthermore, for polymers, the low thermal conductivity becomes an important and critical contribution for obtaining high ZTs. The ionic conducting polymers (ICPs), e.g., polyaniline (PANI) [7,8], polypyrole (PPy) [9], and polythiophene [10–12], along with their high electrical conductivity and intrinsically low thermal conductivity, are considered as the most promising and novel organic TE materials.

Toshima et al. have demonstrated a series of PANI films [13,14], one of the most commonly studied TE polymers, with various dopants and found that some specific dopants

* Corresponding authors. Tel.: +886 3 571 2121x31287; fax: +886 3 572 4727 (C.-H. Chen), tel.: +886 3 571 2121x31873; fax: +886 3 572 4727 (W.-T. Whang).

E-mail addresses: chunhuachen@mail.nctu.edu.tw (C.-H. Chen), wtwhang@mail.nctu.edu.tw (W.-T. Whang).

1566-1199/$ - see front matter © 2011 Elsevier B.V. All rights reserved.
doi:10.1016/j.orgel.2011.09.004

can effectively increase the electrical conductivity to several hundred Siemens per centimeter. However, due to the low Seebeck coefficient, the highest ZT can only reach $\sim 10^{-3}$ around room temperature, which is still insufficiently high for practical application. The ICPs with specific dopants indeed provide the excellent and stable electric conductivities needed, but it is generally difficult to obtain a high Seebeck coefficient simultaneously. A significant enhancement in ZT has been achieved by synthesizing specially designed copolymers with a high electrical conductivity, e.g., poly(2,5-dimethoxyphenylenevinylene-co-phenylenevinylene) and poly(2,5-diethoxyphenylenevinylene-co-phenylenevinylene), which exhibit a greatly improved ZT of $\sim 10^{-2}$ and $\sim 10^{-1}$, respectively [15,16].

As a popular commercial conducting polymer, the water-dispersible poly(3,4-ethylenedioxythiophene):poly (styrenesulfonate) (PEDOT:PSS) has become one of the most promising conductive polymers and has been widely applied in modern photoelectronic devices [17]. The TE investigations for PEDOT:PSS can be traced back to 2002, when Kim et al. established that the Seebeck coefficient decreases with the addition of the dielectric solvent of dimethyl sulfoxide (DMSO) [10]. The topic began to attract growing interest until in 2009 numerous results were published regarding both as-received PEDOT:PSS and blended composites [10–12,18]. Although the addition of DMSO has been widely accepted as an effective approach to greatly increase the electrical conductivity by several orders of magnitude, in the meantime, the Seebeck coefficient also drastically decreases, even with a very small addition, e.g., 0.5 wt.%, and seems to have less change with the variation of the DMSO concentration [11].

Due to the difficulty of independently controlling the Seebeck coefficient and electrical conductivity, blending of different organic/inorganic TE materials provides a simple and potential way to individually optimize these two parameters of the blended TE composites. For instance, Zhang et al. have demonstrated one design of organic–inorganic hybrid films, i.e., one Bi_2Te_3 granular layer coated with one thick PEDOT:PSS layer, and obtained a power factor of $\sim 16\ \mu W/mK^2$, which is much lower than their theoretical prediction using a simplified ideal model [12]. See et al. have also presented an in situ synthesis of the composite of the Te nanorods and PEDOT:PSS, which has a maximum Seebeck coefficient of 163 μV/K and power factor of $\sim 70\ \mu W/mK^2$ [18]. All these hybrid results indicate that no matter whether the TE heteromaterials are integrated in parallel or serial methods, the final TE performance is directly correlated with that of the individual components [12]. It is thus of great importance and meaningful to make efforts to enhance the TE performance of all components, especially the polymers, such as the PEDOT:PSS polymers in the above cases.

In this paper, the effects of the ammonium formate (AF) dopants on the Seebeck coefficient, electrical conductivity, power factor and microstructures of the commercial PEDOT:PSS films are presented. It has been reported that AF can cut off alkyl groups or side chains from benzene [19]. The results motivated us to examine if AF can be a promising dopant to effectively tune the electrical properties of conducting polymers. In addition, since AF will decompose into formamide and water with the presence of heat [20], in our experience, a two-step drying process was specially designed to form PEDOT:PSS films with nano/micro-fractures in which significant phonon scattering may occur, reducing the thermal conductivity of the films. During the first drying step at lower temperature, the only solvent, water, will be gently removed to create dried AF blended PEDOT:PSS films and a very small fraction of the AF dopants will also decompose into the gas phase. The following higher-temperature step will make the trapped solid AF dopants almost decompose to simultaneously form open or closed voids or channels randomly distributed over the films.

2. Experiment

Commercial PEDOT:PSS and AF were purchased from H.C. Starck (Clevios PH 500, 1.0–1.4 wt.%) and Showa Chemical Inc., respectively, and used without further purification. The received PEDOT:PSS solution was doped with 5, 10, 20 and 50 wt.% AF, and respectively denoted as P5, P10, P20, and P50. It must be noted that the weight percentages mentioned above are expressed only by the respective weight percentages of the solid content irrespective of the water solvent, not the whole solution mixture. The 5 wt.% DMSO doped and raw PEDOT:PSS solutions were also prepared for comparison. The chemical structures are shown in Fig. 1. The glass slides were cut into $2.5 \times 2.5\ cm^2$ pieces as the substrates and washed with ultrasonic cleaning processes in detergent, deionized water, and isopropyl alcohol, sequentially. An approximate 100 μL of each prepared PEDOT:PSS solution was dropped onto the as-cleaned glass substrate using a micropipette and spread evenly. The deposited sample was firstly dried in air at 40 °C for 1 h mainly to drive off the H_2O solvent and then kept at 80 °C for another 1 h to further remove the residual solvent as well as to evaporate the AF dopants.

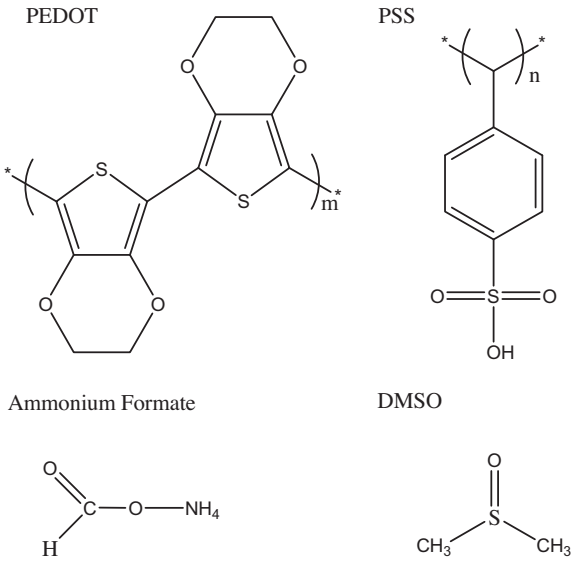

Fig. 1. Chemical structures of PEDOT, PSS, AF, and DMSO.

The final thickness of each dried PEDOT:PSS film was in the range of ~4–6 μm.

The sheet resistance and the electrical conductivity were measured with an automated four-point probe system (Resistest RT-80/Resistage RT-80, Napson Corporation). The corresponding carrier concentration and Hall mobility were characterized with a Hall system (Accent HL5500). The cross-section SEM images provided the accurate thicknesses needed. For the Seebeck coefficient measurement, a maximum temperature gradient of 10 °C was created between two electrodes with an interval of 1.0 cm. The Seebeck voltage and temperature difference were recorded in situ for obtaining the Seebeck coefficients. The samples for the scanning electron microscope (SEM; JSM-6500, JEOL) were broken in liquid nitrogen to avoid plastic deformation of the films. Thermogravimetry analysis (TGA, Q500, TA instruments) was deployed not only to understand the decomposition process of AF but also to characterize the thermostability of the produced films. All TGA samples were pre-heated at 40 °C for 10 min. The time-resolved decomposition of the as-received AF powders at 80 °C and the temperature-dependent weight loss of the prepared PEDOT:PSS films up to 800 °C were respectively recorded. The furnace chamber was constantly purged with nitrogen to minimize the effect of oxygen and to serve as a carrier gas, taking waste out of the chamber. The UV–Vis absorption spectra were recorded with a UV–Vis spectrophotometer (Evolution 300, Thermo Scientific). Thermal conductivity was analyzed by placing a free-standing polymer film between two stacking copper pillars. A heat source generates heat from the bottom of the lower pillar and heat flows upward, through the sample, and then into the upper pillar. Temperatures were measured at certain points of the two pillars to calculate the speed of the heat flow and thermal conductivity of the polymer film.

3. Results and discussion

Fig. 2 shows the cross-section and top-view SEM images of the unmodified and AF-doped PEDOT:PSS films, respectively. In contrast to the very smooth and flat surface of the unmodified PEDOT:PSS, the surface roughness as well as the morphological defect within the film, e.g., the cracks, voids and column structures, obviously increase with the increase of the AF dopant, especially when the AF exceeds 20 wt.%. It is difficult to spread the PEDOT:PSS solution with AF dopants over 50 wt.% since the strong ionic interaction among the AF salts will make the solution gel.

In order to identify the role of AF on the fracture structures, TGA analysis was performed on the as-received AF powders to understand its decomposition behavior. As can be seen in Fig. 3(a), the weight of the AF powders decreases approximately as a linear function with the heating time at 80 °C and approaches complete decomposition after 100 min. It is thus clear that the structural fractures of the PEDOT:PSS films as observed in Fig. 2 were mainly created

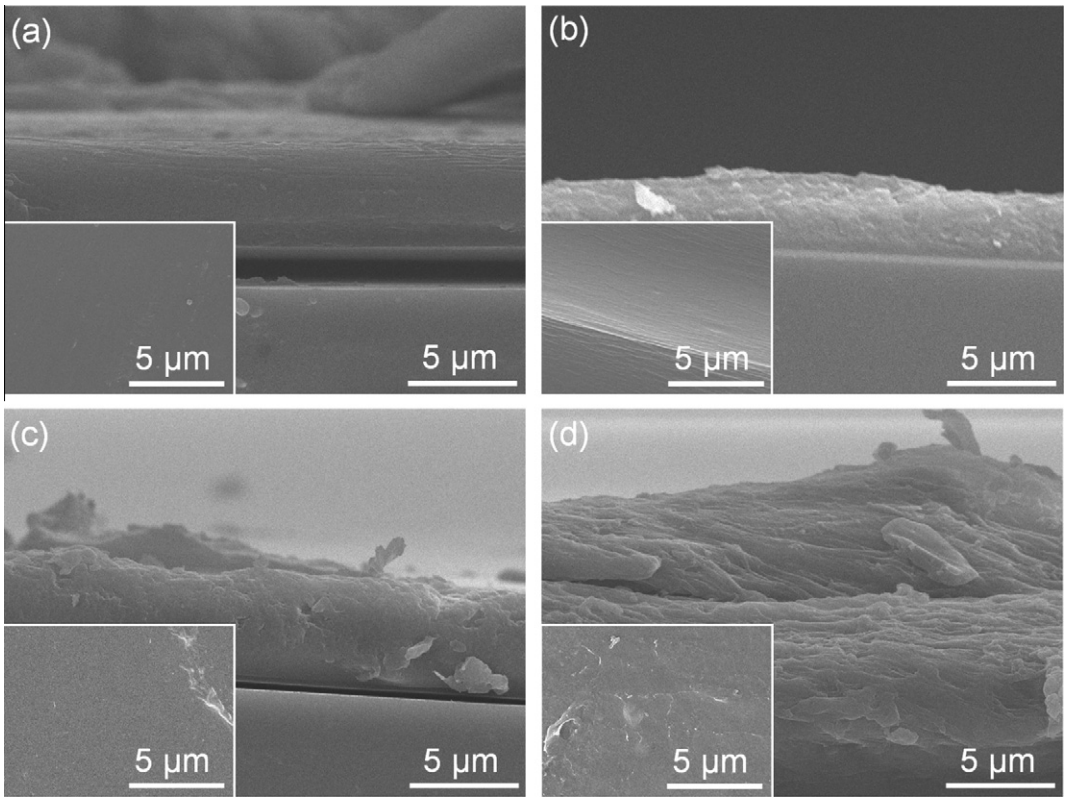

Fig. 2. The cross-section and top-view (inset) SEM images of (a) PH 500, (b) P10, (c) P20, and (d) P50. (e) Image of the close-up of the crack formed during sample preparation.

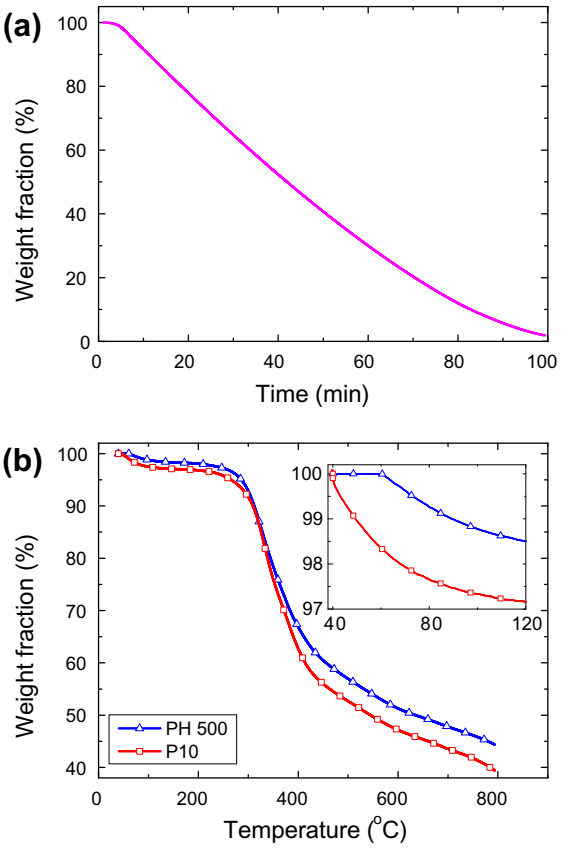

Fig. 3. TGA curves of (a) as-received AF powders and (b) PH 500 and P10.

during the second drying process, i.e., 80 °C for 60 min, due to the violent decomposition of AF at this condition. Because of the lower mechanical strength of the PEDOT:PSS film, the decomposition gas will be released toward the film surface or just trapped in the films. When the three-dimensional pores or channels are open to atmosphere, the inner gas will be exhausted by the gravity of the PEDOT:PSS films to form collapsed two-dimensional interfaces.

Fig. 3(b) is the temperature dependence of the weight loss of PH 500 and P10 from 40 to 800 °C. Basically, the TGA curves for PH 500 and P10 are quite similar to our expectation, since PH 500 is the only main component for both cases. A drastic weight loss of P10 found at the very beginning stage up to ~100 °C should originate from the further decomposing of the residual AF, as discussed above. As can be seen, at 80 °C, i.e., the temperature of the second drying step, the weight loss difference between PH 500 and P10 remains at less than 1.5%, indicating the possible residual level of AF. The adding of AF seems not to affect the thermostability of the PH 500 films. As displayed, the substantial decomposition for both PH 500 and P10 found at ~300 °C is close to that for traditional Polyimide (PI), which is commonly used for flexible substrates in electronic devices. Therefore, the thermostability of the present AF-doped PH 500 film is sufficient for future applications of the soft thermoelectric devices.

Table 1
Seebeck coefficients (S), sheet resistances (R), electrical conductivities (σ), and power factors (P) of the as-received and modified PEDOT:PSS films.

	R (Ω/□)	σ (S/cm)	S (μV/K)	P (μW/mK^2)
PH 500	825.57	1.21	12.4	0.019
DMSO-doped	2.93	524.30	11.6	7.06
P5	21,590	0.11	30.6	0.010
P10	619,100	0.019	220.0	0.092
P10′	323,640	0.036	436.3	0.69

P10′:P10 solution stored at 10 °C for 1 month.

Table 2
Carrier concentrations (n), Hall mobilities (μ_H), and calculated electrical conductivities (σ_H) of the as-received and modified PEDOT:PSS films.

	n (cm^{-3})	μ_H (cm^2/Vs)	σ_H (S/cm)
PH 500	5.5×10^{18}	2.96	2.64
DMSO-doped	1.1×10^{21}	3.81	670
P10	4.3×10^{17}	1.43	0.0984

Table 1 summarizes the measured thermoelectric properties of the as-received and modified PEDOT:PSS films. The most notable changes are that the electrical conductivity of the AF doped film decreases by one to two orders of magnitude compared to the unmodified PH 500. For further evaluation of the electrical conductivity, Hall measurements were carried out and the results confirmed that all the prepared films were hole-type carrier domination. In the p-type semiconductors, the electrical conductivity σ can be expressed by the relationship:

$$\sigma = e\, n\, \mu_H \tag{2}$$

where e, n, and μ_H is the electronic charge, carrier concentration, and Hall mobility, respectively. As can be seen in Table 2, the electrical conductivity of the pristine and modified PEDOT:PSS films obtained from the product of these two competing factor, n and μ_H, is of the same order of magnitude as that measured by 4-point probe method as shown in Table 1, indicating the reliability of the present measurements. Obviously, the largely decreased electrical conductivity of the AF doped PEDOT:PSS film (P10), was mainly caused by the one-order-of-magnitude reduction in the carrier concentration. This probably results from the interaction between the AF molecules and PSS monomers, and thus inhibits the role of the carrier supplier of PSS for PEDOT. Checking the results in Table 2, the Hall mobility shows relatively less variation (<50%) with dopants, either the DMSO or the AF.

In addition to the electrical conductivity, it is noteworthy that the Seebeck coefficient for P10 as displayed in Table 1 is ~20 times higher than that for as-received PH 500 as well as the widely-synthesized DMSO-modified PH 500. Generally, the Seebeck coefficient will be affected, either increasing or decreasing, even with only slight doping, e.g., the DMSO, but will not effectively vary with the doping concentration. It is surprising in the present case that the Seebeck coefficient significantly enhances with the AF doping concentration.

A theoretical derivation of Seebeck coefficient (S) is expressed as [21]:

$$S(T) = \frac{1}{eT}\frac{\int [E_F(T) - E]\delta\sigma(E)dE}{\int \delta\sigma(E)dE} \quad (3)$$

where E_F is the Fermi level and $\delta\sigma(E)$ the differential conductivity at energy E. This equation holds for both band and hopping transport. With the further assumption of unipolar charge carrier transport at one narrow transport level (E_T), Eq. (3) can be written as:

$$S(T) = \frac{E_F(T) - E_T}{eT} \quad (4)$$

The energy difference E_F(T)−E_T is correlated to the carrier concentration as well known [22]. The variation of about one order decrease of the carrier concentration will great increase the $E_F(T)$−E_T, and thus enhance the Seebeck coefficient according to Eq. (4). Similar tendency between the carrier concentration and thermoelectric properties, including the electrical conductivity and the Seebeck coefficient can also be observed in doped organic semiconductors [21].

In addition to the direct evidence of the carrier concentration influence on the electrical conductivity and Seebeck coefficient, here we further consider another phenomenon that might happen in the present AF doped system and affect these two parameters, σ and S. It has been reported that AF can substitute double bonds sites and cut off side groups with the presence of catalysts [19,23,24]. Thus, it is reasonable to consider that the double bonds on PEDOT will be partially damaged by AF. The conjugation length of PEDOT will thus be reduced and the lowered density of states of the conducting bands and valence bands lead to a wider band gap. Martin et al. have experimentally proven the correlation between the conjugation length and the band gap by analyzing UV–Vis spectra of samples with a precisely controlled conjugation length from one oligomer to six oligomers. They found that the UV–Vis absorption energy E_{abs} (eV) were found to be ruled by the following equation derived from Kuhn's electron gas model [25].

$$E_{abs} = V_0 + \left(\frac{h^2}{4mL_0^2} - \frac{V_0}{4}\right)\frac{1}{N + 0.5} \quad (5)$$

where V_0 is the amplitude which corrects the free electron gas model, h the Plank constant, m the mass of the electron, L_0 the unit length of the conjugation, and N the number of conjugated bonds. Since N is much larger than 0.5 in the present case, the absorption energy E_{abs} shows a linear relation with $1/N$. As a result, the blue shift of the UV–Vis peak should increase with the decreasing of conjugation length. The slight decrease of the Hall mobility of P10 as observed in Table 2 might also be correlated to the possible decrease of conjugation length. The UV–Vis spectra of the prepared films shown in Fig. 4 represent a large blue shift for the AF-doped PH 500, which provides reliable evidence of the widening of the band gaps. As previously discussed, the widened band gap should mainly originate from the great decrease of the carrier concentration of the AF doped films.

According to the definition of the power factor, either increased electrical conductivity or especially the Seebeck coefficient is of great importance to enhance the power factor. However, these two parameters generally cannot be increased simultaneously due to the inverse relation to the gap between E_T and E_F of the material, i.e., when the gap becomes wider, a higher Seebeck coefficient can be obtained, whereas a lower electrical conductivity will be presented. This trade-off has also been one of the major problems for all categories of thermoelectric materials. Although the electrical conductivity decreases by two orders of magnitude due to the doping of 10 wt.% AF (P10), the one order of magnitude increase in the Seebeck coefficient leads to an overall one order increase in the power factor, compared with the pristine PH 500. A similar tendency can also be found in the case of P5.

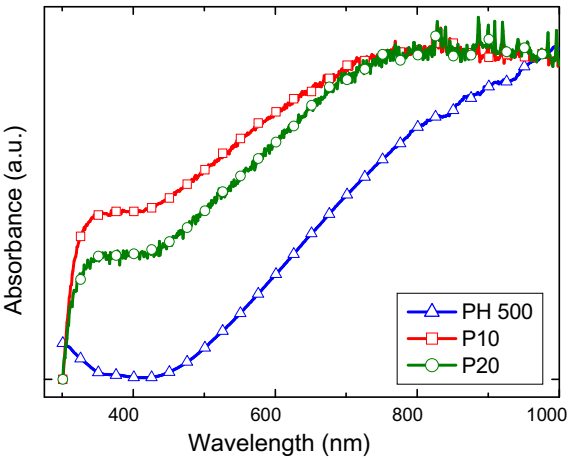

Fig. 4. The normalized UV–Vis absorption spectra of PH 500, P10, and P20.

In order to investigate the AF doping effect on the phonon scattering and to estimate the ZT value, the thermal conductivity of P10′ was measured near the room temperature. The obtained thermal conductivity of 0.18 W/mK is close to that of the PH 500 film with 5% DMSO (0.32 W/mK) [26] and PH 500 pellet with 10% DMSO (0.17 W/mK) [27] been reported. The estimated ZT value of P10′ would thus be 1.1×10^{-3} at room temperature. This result indicates that not only can electrical conductivity modification improve the ZT value, but TE behavior can also be enhanced by modifying the Seebeck coefficient to a comparative value regarding other works.

Another interesting phenomenon is observed that when the prepared AF doped film is stored at lower temperatures (~10 °C) in refrigerator for a period of time, the Seebeck coefficient increases with the storage time. For instance, the Seebeck coefficient of P10 rises from the initial 220 to 436.3 μV/K after 1 month storage. The solution was kept in a refrigerator at all times and only taken out for sample coating. The mechanism of this effect on especially the Seebeck coefficient is not clear so far.

4. Conclusion

In summary, we have successfully incorporated AF into Clevios PH 500 with various concentrations from 5 to 50 wt.% to form continuous films with distinct

thermoelectric properties and microstructures. With the increase of the AF doping, the Seebeck coefficient discernibly varied in a pretty wide range in which a maximum of 436.3 μV/K was found for 10 wt.% AF (P10′), i.e., ~40 times greater in magnitude, compared with 12.4 μV/K for pure PH 500. The greatly increased Seebeck coefficient, as well as the accompanying decreased electrical conductivity, probably originates from the reduction of the conjugation length of PEDOT by AF, as evidenced by the UV–Vis spectra. The best power factor obtained is 0.69 $\mu W/mK^2$, which is one order higher than that of pristine PH 500, but it is still lower than PH 500 blend with 5 wt.% DMSO, due to its lack of electrical conductivity. Nevertheless, this work provides a new procedure to increase the Seebeck coefficient of the polymer by simple blending, which has not previously been reported. In addition, AF also plays an important role in the formation of the closed or open pores and channels by thermal decomposing of AF, as can be seen in SEM images. These nano/micro-defects are considered to effectively scatter phonons and thus to further enhance the thermoelectric performance.

References

[1] D.M. Rowe (Ed.), CRC Handbook of Thermoelectrics, CRC Press, Boca Raton, 1995.

[2] J.P. Fleurial, A. Borshchevsky, T. Caillat, R. Ewell, New materials and devices for thermoelectric applications, Annu. Meet. – Am. Inst. Chem. Eng. 2 (1997) 1080–1085.

[3] J. Wüsten, K. Potje-Kamloth, Organic thermogenerators for energy autarkic systems on flexible substrates, J. Phys. D 41 (2008) 135113.

[4] R.B. Aïch, N. Blouin, A. Bouchard, M. Leclerc, Electrical and thermoelectric properties of poly(2,7-carbazole) derivatives, Chem. Mater. 21 (2009) 751–757.

[5] H.J. Goldsmid, R.W. Douglas, The use of semiconductors in thermoelectric refrigeration, Br. J. Appl. Phys. 5 (1954) 386–390.

[6] C.J. Vineis, A. Shakouri, A. Majumdar, M.G. Kanatzidis, Nanostructured thermoelectrics: big efficiency gains from small features, Adv. Mater. 22 (2010) 3970–3980.

[7] F. Yakuphanoglu, B.F. Şenkal, A. Saraç, Electrical conductivity, thermoelectric power, and optical properties of organo-soluble polyaniline organic semiconductors, J. Electron. Mater. 37 (2008) 930–934.

[8] F. Yakuphanoglu, B.F. Şenkal, Electronic and thermoelectric properties of polyaniline organic semiconductor and electrical characterization of Al/PANI MIS diode, J. Phys. Chem. C 111 (2007) 1840–1846.

[9] K. Bender, E. Gogu, I. Hennig, D. Schweitzer, H. Müenstedt, Electric conductivity and thermoelectric power of various polypyroles, Synth. Met. 18 (1987) 85–88.

[10] J.Y. Kim, J.H. Jung, D.E. Lee, J. Joo, Enhancement of electrical conductivity of poly(3,4-ethylenedioxythiophene)/poly(4-styrenesulfonate) by a change of solvents, Synth. Met. 126 (2002) 311–316.

[11] K.C. Chang, M.S. Jeng, C.C. Yang, Y.W. Chou, S.K. Wu, M.A. Thomas, Y.C. Peng, The thermoelectric performance of poly(3,4-ethylenedioxythiophene)/poly(4-styrenesulfonate) thin films, J. Electron. Mater. 38 (2009) 1182–1188.

[12] B. Zhang, J. Sun, H.E. Katz, F. Fang, R.L. Opila, Promising thermoelectric properties of commercial PEDOT:PSS materials and their Bi_2Te_3 powder composites, ACS Appl. Mater. Inter. 2 (2010) 3170–3178.

[13] N. Toshima, H. Yan, M. Kajita, Y. Honda, N. Ohno, Novel synthesis of polyaniline using iron(III) catalyst and ozone, Chem. Lett. 29 (2000) 1428–1429.

[14] H. Yan, N. Sada, N. Toshima, Thermal transporting properties of electrically conductive polyaniline films as organic thermoelectric materials, J. Therm. Anal. Calorim. 69 (2002) 881–887.

[15] Y. Hiroshige, M. Ookawa, N. Toshima, High thermoelectric performance of poly(2,5-dimethoxyphenylenevinylene) and its derivatives, Synth. Met. 156 (2006) 1341–1347.

[16] Y. Hiroshige, M. Ookawa, N. Toshima, Thermoelectric figure-of-merit of iodine-doped copolymer of phenylenevinylene with dialkoxyphenylenevinylene, Synth. Met. 157 (2007) 467–474.

[17] O.F. Yilmaz, S. Chaudhary, M. Ozkan, A hybrid organic–inorganic electrode for enhanced charge injection or collection in organic optoelectronic devices, Nanotechnology 17 (2006) 3662–3667.

[18] K.C. See, J.P. Feser, C.E. Chen, A. Majumdar, J.J. Urban, R.A. Segalman, Water-processable polymer–nanocrystal hybrids for thermoelectrics, Nano Lett. 10 (2010) 4664–4667.

[19] N.C. Ganguly, S. Dutta, M. Datta, Mild and efficient deprotection of allyl ethers of phenols and hydroxycoumarins using a palladium on charcoal catalyst and ammonium formate, Tetrahedron Lett. 47 (2006) 5807–5810.

[20] A. Brann, On the preparation of formamide, J. Am. Chem. Soc. 40 (1918) 793–796.

[21] A. Nollau, M. Pfeiffer, T. Fritz, K. Leo, Controlled n-type doping of a molecular organic semiconductor: naphthalenetetracarboxylic diabhydride (NTCDA) doped with bis(ethylenedithio)–tetrathiafulvalene (BEDT–TTF), J. Appl. Phys. 87 (2000) 4340–4343.

[22] S.M. Sze, Kwok K. Ng, Physics of Semiconductor Devices, third ed., John Wiley and Sons, America, 2007 (Section 1.4).

[23] S. Gowda, K. Abiraj, D.C. Gowda, Reductive cleavage of azo compounds catalyzed by commercial zinc dust using ammonium formate or formic acid, Tetrahedron Lett. 43 (2002) 1329–1331.

[24] B.C. Ranu, A. Sarkar, Regio- and stereoselective hydrogenation of conjugated carbonyl compounds via palladium assisted hydrogen transfer by ammonium formate, Tetrahedron Lett. 35 (1994) 8649–8650.

[25] R.E. Martin, U. Gubler, C. Boudon, V. Gramlich, C. Bosshard, J.P. Gisselbrecht, P. Günter, M. Gross, F. Diederich, Poly(triacetylene) oligomers: characterization, and estimation of the effective conjugation length by electrochemical, UV/Vis, and nonlinear optical methods, Chem. Eur. J. 3 (1997) 1505–1512.

[26] M. Scholdt, H. Do, J. Lang, A. Gall, A. Colsmann, U. Lemmer, J.D. Koenig, M. Winkler, H. Boettner, Organic semiconductors for thermoelectric applications, J. Electron. Mater. 39 (2010) 1589–1592.

[27] F.X. Jiang, J.K. Xu, B.Y. Lu, Y. Xie, R.J. Huang, L.F. Li, Thermoelectric performance of poly(3,4-ethylenedioxythiophene):poly(styrenesulfonate), Chin. Phys. Lett. 25 (2008) 2202–2205.